The EMBO Journal Vol. 20 No. 24 pp. 6958–6968, 2001

A highly selective telomerase inhibitor limiting human cancer cell proliferation

Klaus Damm[1,2], Ulrike Hemmann[3,4], Pilar Garin-Chesa[2], Norbert Hauel[5], Iris Kauffmann[5], Henning Priepke[5], Claudia Niestroj[2], Christine Daiber[2], Barbara Enenkel[2], Bernd Guilliard[2], Ines Lauritsch[2], Elfriede Müller[2], Emanuelle Pascolo[2], Gabriele Sauter[2], Milena Pantic[6,7], Uwe M.Martens[6], Christian Wenz[8], Joachim Lingner[8], Norbert Kraut[3], Wolfgang J.Rettig[9] and Andreas Schnapp[2]

Boehringer Ingelheim Pharma KG, [2]Oncology Research, [3]Genomics, [5]Chemistry, Birkendorfer Strasse 65, D-88397 Biberach, [6]University Medical Center, Department for Hematology/Oncology, Hugstetterstrasse 55, D-79106 Freiburg i. Br., [7]Albert-Ludwigs-University, Department of Biology, D-79106 Freiburg i. Br., Germany, [8]Swiss Institute for Experimental Cancer Research (ISREC), CH-1066 Epalinges, Switzerland and [9]Boehringer Ingelheim Austria GmbH, Dr. Boehringer-Gasse 5–11, A-1120 Vienna, Austria

[4]Present address: Aventis Pharma GmbH, Fraunhofer Strasse 13, D-82152 Martinsried, Germany

[1]Corresponding author
e-mail: klaus.damm@bc.boehringer-ingelheim.com

Telomerase, the ribonucleoprotein enzyme maintaining the telomeres of eukaryotic chromosomes, is active in most human cancers and in germline cells but, with few exceptions, not in normal human somatic tissues. Telomere maintenance is essential to the replicative potential of malignant cells and the inhibition of telomerase can lead to telomere shortening and cessation of unrestrained proliferation. We describe novel chemical compounds which selectively inhibit telomerase *in vitro* and *in vivo*. Treatment of cancer cells with these inhibitors leads to progressive telomere shortening, with no acute cytotoxicity, but a proliferation arrest after a characteristic lag period with hallmarks of senescence, including morphological, mitotic and chromosomal aberrations and altered patterns of gene expression. Telomerase inhibition and telomere shortening also result in a marked reduction of the tumorigenic potential of drug-treated tumour cells in a mouse xenograft model. This model was also used to demonstrate *in vivo* efficacy with no adverse side effects and uncomplicated oral administration of the inhibitor. These findings indicate that potent and selective, non-nucleosidic telomerase inhibitors can be designed as novel cancer treatment modalities.

Keywords: cancer/inhibitor/microarray/senescence/telomerase

Introduction

Telomerase is a cellular RNA-dependent DNA polymerase that serves to maintain the tandem arrays of telomeric TTAGGG repeats at eukaryotic chromosome ends (Morin, 1989; Blackburn and Greider, 1995). In human cells, the enzyme comprises a high molecular weight complex with a template-containing RNA subunit (Feng *et al*., 1995) and protein components including the catalytic subunit human telomerase reverse transcriptase, hTERT (Harrington *et al*., 1997; Meyerson *et al*., 1997; Nakamura *et al*., 1997). Telomerase activity has been demonstrated in immortalized cell lines and in 80–90% of human cancer specimens representing a range of cancer types (Counter *et al*., 1994; Kim *et al*., 1994; Shay and Bacchetti, 1997) and recently, human telomerase has been directly implicated in cellular immortalization and tumorigenesis (Bodnar *et al*., 1998; Hahn *et al*., 1999a). In most normal human cells, telomerase activity is low or not detectable, and telomeric DNA is progressively lost at a rate of 30–120 bp with each replication cycle (Harley *et al*., 1990; Hastie *et al*., 1990; Counter *et al*., 1992). Eventually, telomeres shorten to a critical length and lose their ability to protect the ends of chromosomal DNA (Counter *et al*., 1992; Blasco *et al*., 1997). Uncapped chromosomes are sensitive to degradation and fusion and can activate DNA damage checkpoints, thus potentially contributing to the replicative senescence and growth arrest observed in aged primary cultured cells (Hayflick and Moorhead, 1961). Indeed, it has been proposed that telomere length specifies the number of cell divisions a cell can undergo prior to senescence (Cooke and Smith, 1986; Harley, 1991). In cancer cells, the reactivation of telomerase is thought to stabilize telomere length, thereby compensating for the cell division-related telomere erosion and providing unlimited proliferative capacity to malignant cells (Counter *et al*., 1992; Kim *et al*., 1994). As a corollary to this hypothesis, the inhibition of telomerase in tumour cells should disrupt telomere maintenance and return malignant cells to proliferative crisis followed by senescence or cell death (Harley *et al*., 1990; Counter *et al*., 1992). Genetic experiments using a dominant-negative form of human telomerase demonstrated that telomerase inhibition can result in telomere shortening followed by proliferation arrest and cell death by apoptosis (Hahn *et al*., 1999b; Zhang *et al*., 1999).

A challenge for the development of pharmaceutically useful telomerase inhibitors is the long lag period required to observe telomere attrition. Cellular growth arrest that depends on telomere shortening will require a series of cell division cycles to become apparent, and treatment may have to be given continuously for weeks to months, potentially in conjunction with other treatment modalities. Therefore, potency of action, selectivity, tolerability and

suitable pharmaceutical formulations are formidable tasks to be met in telomerase drug design. Here we describe a novel structural class of non-peptidic, non-nucleosidic inhibitors of human telomerase that are highly potent and selective *in vitro* and pharmacologically active in the control of human cancer cell proliferation.

Results

Small molecules selectively inhibit telomerase activity in vitro

To characterize small-molecule inhibitors of human telomerase, we used nuclear extracts prepared from HeLa cells to set up an *in vitro* telomerase activity assay (Morin, 1989; Schnapp *et al*., 1998). Our study focuses on compounds with the general structure shown in Figure 1A, for which systematic structure-activity correlations have been established (N.Hauel *et al*., manuscript in preparation). Two examples from this class of compounds, designated BIBR1532 {2-[(E)-3-naphtalen-2-yl-but-2-enoylamino]-benzoic acid} and BIBR1591 {5-morpholin-4-yl-2-[(E)-3-naphtalen-2-yl-but-2-enoylamino]-benzoic acid}, inhibit the *in vitro* processivity of telomerase in a dose-dependent manner, with half-maximal inhibitory concentrations (IC_{50}) of 93 and 470 nM, respectively (Figure 1B). The selectivity of BIBR1532 was assessed in a panel of DNA and RNA polymerases, including HIV reverse transcriptase, showing that none of these enzymes was inhibited at concentrations vastly exceeding the IC_{50} for telomerase (Figure 1C). As shown in the direct telomerase assay (Figure 1D), BIBR1532 can also inhibit recombinant, affinity purified telomerase, suggesting that it is indeed the catalytic activity of the telomerase enzyme which is the target for BIBR1532 inhibition.

Telomerase inhibitors induce telomere shortening in cancer cells

The compounds also had no effect on short-term cell viability or proliferation, as determined in a 7 day cytotoxicity assay using concentrations 100-fold above the *in vitro* IC_{50} (i.e. 10 μM for BIBR1532, 50 μM for BIBR1591). To investigate the cellular consequences of long-term treatment with a telomerase inhibitor, we cultivated exponentially growing NCI-H460 lung carcinoma cells in the presence of BIBR1532 (10 μM) or BIBR1591 (50 μM), respectively. As a control, untreated cells or cells treated with the solvent alone were grown using the same culture conditions. Periodically, total DNA samples were prepared from treated and control cells, digested with frequently cutting restriction enzymes and the telomere length examined by Southern blotting. NCI-H460 cells exhibit a heterogeneous size distribution, with an average telomere length of 4 kb and a predominant range of 2 to 6 kb (Figure 2A). As cells are propagated in

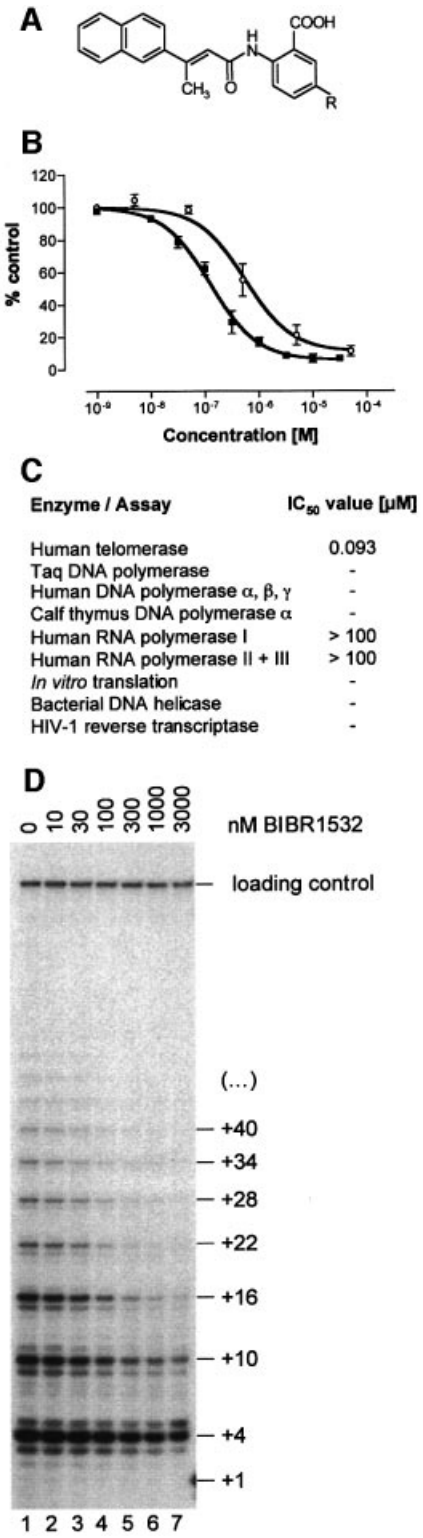

Fig. 1. Specific and selective telomerase inhibitors. (**A**) Chemical structure of the BIBR compound class of inhibitors. BIBR1532, R = H; BIBR1591, R = morpholin-4-yl. (**B**) Dosis-dependent inhibition of telomerase activity by BIBR1532 (solid squares) and BIBR1591 (open circles). Assays were performed and quantified using a PCR-based protocol followed by a TCA precipitation step. The incorporated activity of samples with inhibitor was normalized to the control and plotted against the inhibitor concentration. (**C**) Selectivity profile of BIBR1532. Enzymatic activity was assayed in the presence of 0–50 μM BIBR1532 as described in Materials and methods. –, no effect at 50 μM. (**D**) Direct assay of telomerase activity. Telomerase was reconstituted with insect cell expressed hTERT and *in vitro* transcribed RNA, affinity purified and incubated in the presence of different concentrations of BIBR1532. Telomerase products were separated on a sequencing gel.

the presence of telomerase inhibitor, steady telomere shortening occurred. The average telomere restriction fragment (TRF) size shortened progressively from 4 to 1.5 kb at population doubling (PD) 140 (Figure 2A), corresponding to a telomere loss of 30 bp/PD. We observed a comparable erosion of the telomeres in HT1080 fibrosarcoma, MDA-MB231 breast carcinoma and DU145 prostate carcinoma cells similarly treated with telomerase inhibitor (Figure 2A). In contrast, untreated cells or cells exposed to solvent alone maintained a stable TRF size (Figure 2A).

Telomerase inhibitors limit cancer cell proliferation

The growth kinetics of inhibitor-treated cells initially did not differ from those of untreated or solvent treated control cells, regardless of the cell line used. NCI-H460 cell cultures in the absence or presence of telomerase inhibitor exhibited no or only minor differences in proliferation for more than 120 days of treatment (Figure 2B). However, after PD135 the inhibitor-treated cells slowed their growth and showed an almost complete inhibition of proliferation after additional 4–8 population doublings (Figure 2B). This telomerase inhibitor-induced growth arrest is apparently independent of functional p53 since similar growth curves, with an onset of cellular growth arrest after a significant lag-phase, were obtained for the p53-deficient HT1080, MDA-MB231 and DU145 cell lines (Figure 2B). The reduced proliferation capacity of telomerase-inhibited cells near growth arrest was further substantiated in colony formation assays, with about 50% reduction in colony formation for treated versus mock-treated NCI-H460 and HT1080 cells. As a control for compound specificity we also cultivated telomerase-negative, normal human lung fibroblasts as well as an osteosarcoma cell line (SAOS-2) that exhibits the alternative lengthening of telomere (ALT) phenotype (Bryan *et al*., 1995). Our results showed that inhibitor treatment had no effect on telomere length, growth kinetics and morphology for the entire time of treatment (8 weeks) in either cell line.

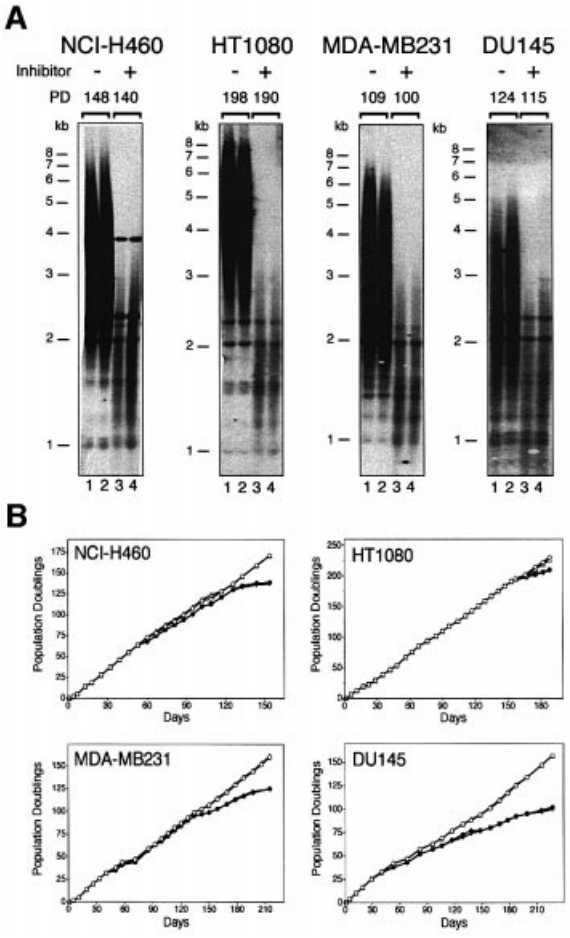

Fig. 2. Telomerase inhibitors induce telomere shortening and limit cell proliferation. (**A**) Total genomic DNA prepared from untreated (lane 1), solvent- (lane 2) or inhibitor-treated (lanes 3 and 4) NCI-H460, HT1080, MDA-MB231 or DU145 cells was assessed for telomere restriction fragment size by Southern blot analysis with a telomeric probe. PD, population doubling; –, absence and +, presence of BIBR1532 or BIBR1591. (**B**) NCI-H460, HT1080, MDA-MB231 and DU145 cells were plated in 24-well plates in duplicate in the presence of 10 μM BIBR1532 or 50 μM BIBR1591 dissolved in 0.1% DMSO (closed symbols). Control cells were untreated (open triangles) or treated with corresponding solvent concentrations (open circles). Cultures were replated every 2–3 days to maintain log-phase growth and to calculate the growth rate.

Reversibility of inhibition

In parallel cultures of the NCI-H460 cells shown in Figure 2B we observed very slowly proliferating cells that were overgrowing the resting, senescent cells in the culture plate, resulting in a flat but measurable growth rate (Figure 3A). Apparently, the treated cells enter senescence not in a parallel but rather in a sequential fashion, which may be due to the heterogeneity of their telomere lengths. We never observed spontaneous telomere lengthening or telomerase-independent growth attributable to the induction of an ALT phenotype. To determine the effect of inhibitor depletion, we transferred the treated cells to normal medium without drug starting at day 220. After a short delay of 3–4 days the cells exhibited a growth rate similar to the control culture (Figure 3A). Examination of

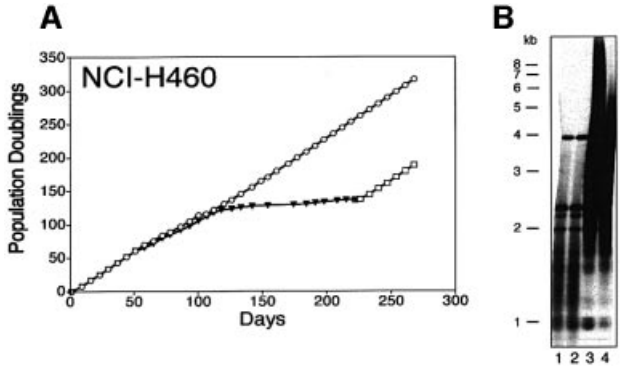

Fig. 3. Reversibility of inhibition. (**A**) NCI-H460 cells were cultivated in 24-well plates in the absence (open circles) or presence of 50 μM BIBR1591 (closed triangles). After 130 days, compound-treated cells were replated only when the culture dishes reached subconfluence. At day 220, these cells were washed, replated in medium without compound and the growth rate monitored for additional 50 days (open squares). (**B**) The median TRF size of inhibitor-treated NCI-H460 cells at day 220 corresponds to only 1.5 kb (lanes 1 and 2). Removal of the inhibitor and cultivation of these cells for 40 PD in absence of inhibitor leads to a significant telomere elongation (lane 3). Untreated control cells at day 260 are also shown for comparison (lane 4).

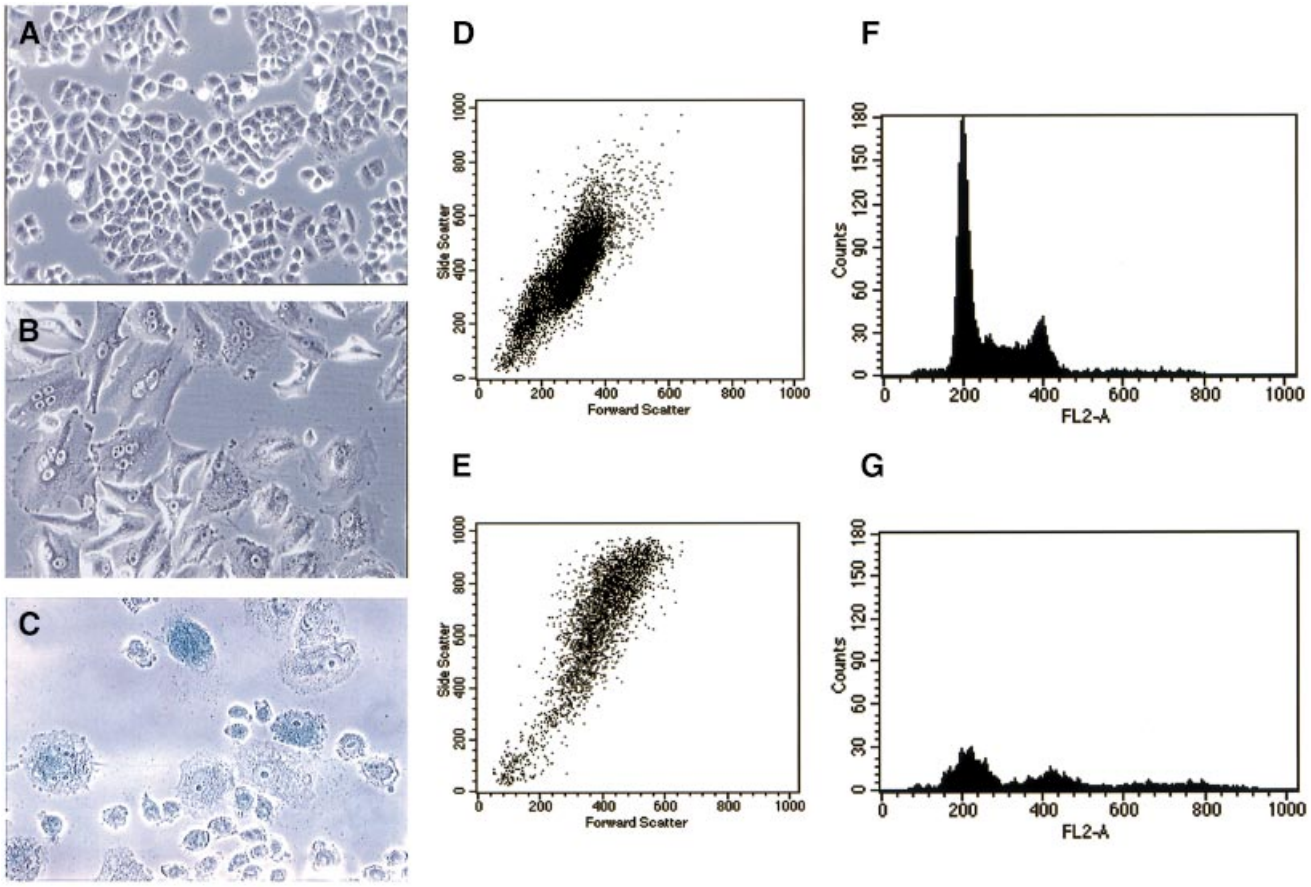

Fig. 4. Induction of a senescence phenotype. Phase contrast micrographs show the cellular morphology of (**A**) untreated and (**B**) inhibitor-treated NCI-H460 cells at PD162 and PD130, respectively. (**C**) Inhibitor-treated NCI-H460 cells from a separate inhibition experiment were stained for β-galactosidase activity at pH 6.0. Phenotypic changes in this experiment were already observed at PD72. (**D**–**G**) Flow cytometric analysis of NCI-H460 cells shown in (C). Dot density maps of PI-staining (*x*-axis) and 90-degree light scatter (*y*-axis) are shown for control (D), and inhibitor-treated cells (PD72) (E). DNA content analysis of control (F), and inhibitor-treated cells (PD72) (G).

the TRF sizes also revealed a rapid elongation of the telomeres in these cells (Figure 3B), demonstrating that the telomerase inhibition is fully reversible.

Telomerase inhibitors induce a senescent phenotype

The inhibitor-treated, late passage tumour cells showed distinctive morphological features associated with senescence of aged normal human cells. In contrast to untreated cell cultures (Figure 4A), the growth-arrested NCI-H460 cells (Figure 4B) became enlarged, often contained multiple nuclei, had a vacuolated cytoplasm and showed induction of senescence associated β-galactosidase activity (Figure 4C). Similar morphological alterations were observed with late-passage HT1080, MDA-MB231 and DU145 cells (data not shown). FACS analysis of inhibitor-treated NCI-H460 cells revealed an elevated forward and side scatter relative to untreated cells, which may reflect increased cell size and granularity (Figure 4D and E). The inhibitor-treated NCI-H460 cells also showed a heterogeneous cell cycle profile, with broad 2n and 4n peaks and a shift towards higher DNA content (Figure 4F and G). We performed extensive FACS analysis and TUNEL staining in p53 positive (NCI-H460) or p53 negative (HT1080, DU145, MDA-MB231) cell lines at different timepoints, but could not detect an increase in apoptosis comparing treated and control cells.

Inhibitor-treated cells exhibit telomere dysfunction

We next analysed chromosomal metaphase spreads derived from late-passage NCI-H460 cells. Due to the reduced proliferative capacity and the correspondingly low mitotic index only eight metaphases were obtained from the inhibitor-treated cells, and these were compared qualitatively with 20 metaphases from control cultures. The loss of telomeric sequences was readily detected using the Q-FISH technique with a telomere-specific probe (Figure 5A and B) (Martens *et al*., 1998). Signal intensity, which has been shown previously to correlate directly with the number of TTAGGG repeats, was significantly (p <0.0001) reduced in the inhibitor-treated cells relative to control cells (Figure 5C). The histogram also shows an accumulation of short telomeres and an increased skewness in the distribution of telomere fluorescence

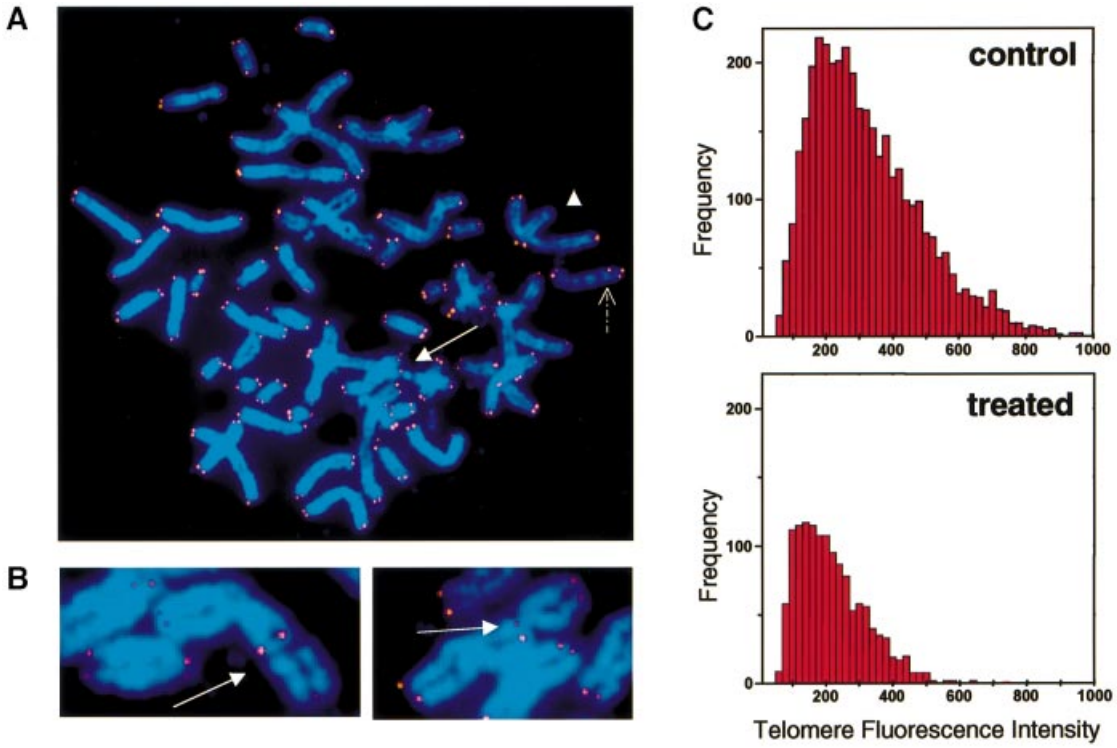

Fig. 5. Telomere analysis of inhibitor-treated NCI-H460 cells. (**A**) Q-FISH analysis of metaphase chromosomes from inhibitor-treated NCI-H460 cells. DAPI-stained chromosomes and Cy-3-labeled telomeres are shown in blue and yellow, respectively. The NCI-H460 cell line is hypotriploid with seven marker chromosomes (modal chromosome number 57) and exhibits a characteristic chromosome with interchromosomal telomere signals. Arrowhead denotes missing telomeres; arrow denotes fused chromosomes; dashed arrow denotes interchromosomal telomere signals. (**B**) Details of end-to-end fusions from another metaphase with telomere signals present at the fusion site. (**C**) Histograms express the fluorescence intensity and frequency of all individual telomere spots from NCI-H460 derived metaphases. Twenty metaphases (n = 3740) were derived from control cultures (PD68) and eight metaphases (n = 1366) were derived from inhibitor treated cells (PD120). n is the number of individual telomere signals. The differences in mean fluorescence intensity (arbitrary fluorescence units ± SD) between the control cells (321 ± 160) and the treated cells (217 ± 101) were highly significant (p <0.0001).

(Figure 5C) which is very similar to the observations in pre-senescent fibroblasts (Martens *et al.*, 2000). Furthermore, we observed an increase in chromosome end fusions (0.88/metaphase in treated versus 0.55/metaphase in control cells) as well as an increased number of chromosomes with no telomere signal at both sister chromatids in treated cells (mean: 3.75/metaphase) compared with control cells (mean: 1.1/metaphase).

Microarray analysis of mRNA expression levels in senescent NCI-H460 cells

To identify genes responsive to pharmacological telomerase inhibition and telomere shortening we determined changes in gene expression levels between inhibitor-treated and untreated NCI-H460 cells using DNA microarrays with the capacity to display transcript levels of 6817 known human genes. Total RNA was prepared from cells exposed to telomerase inhibitor for 7, 28 and 56 days, respectively, or until overt morphological changes characteristic for senescence were apparent. Analysis of the day 7, day 28 and day 56 timepoints revealed only minor variations in RNA transcript patterns without consistent changes. However, in the inhibitor-treated, senescent NCI-H460 cells we identified 302 (4.4%) genes showing at least a 2-fold difference in expression levels in a minimum of three out of four independent comparisons (for complete gene list see Supplementary data available at *The EMBO Journal* Online). The up- or down-regulated genes displaying the largest alterations in expression were assigned to functional categories (Tables I and II).

A large percentage of the 166 down-regulated genes represent proteins involved in cell cycle control, the regulation of DNA synthesis, replication and segregation, and mitosis, as well as transcription and translation processes (Table I). In addition, more than 60 of the 142 up-regulated genes encode lysosomal enzymes, proteins mediating cell-adhesion and growth factors and cytokines with both growth promoting as well as growth inhibitory function (Table II). Only a few of these genes have previously been associated with DNA damage or senescence and most prominent among these is the cyclin-dependent kinase inhibitor $p21^{Waf1}$, which we found to be up-regulated 12.9-fold. In contrast, expression of the breast cancer susceptibility genes BRCA1 and BRCA2 as well as BARD1 (BRCA1-associated Ring domain protein), which are thought to play a key role in the cellular DNA damage response, was found to be repressed. We also observed a 5-fold reduction of hTERT mRNA, encoding the catalytic subunit of telomerase, while the telomere binding protein TRF1 was found among the induced genes. No other genes associated with telomere

Table I. Transcriptional changes induced in NCI-H460 cells by long-term telomerase inhibitor treatment: down-regulation

Accession No.	Fold Δ	Gene name	Identified in context of senescence/ageing
Cell cycle control			
U74612	–11.5	hepatocyte nuclear factor-3/fork head homolog 11A	Ly *et al*. (2000)
X51688	–11.4	cyclin A (*)	Ly *et al*. (2000); Shelton *et al*. (1999)
Z29066	–7.1	NEK2	
X65550	–7.0	mki67a	
X13293	–6.3	B-MYB	Chang *et al*. (2000); Ly *et al*. (2000)
U05340	–4.9	p55CDC	Ly *et al*. (2000)
U33761	–3.9	cyclin A/CDK2-associated p45 (SKP2)	
U77949	–3.5	CDC6-related protein	
M25753	–3.4	cyclin B	Chang *et al*. (2000); Ly *et al*. (2000); Shelton *et al*. (1999)
X54941	–3.3	CKSHS1	Ly *et al*. (2000)
D50914	–3.2	KIAA0124, similar to mouse BOP1	
U65410	–3.1	MAD2	Chang *et al*. (2000)
U01038	–2.9	PLK1	Chang *et al*. (2000); Ly *et al*. (2000)
X05360	–2.5	CDC2	Chang *et al*. (2000); Shelton *et al*. (1999)
U56816	–2.4	MYT1	Ly *et al*. (2000)
X54942	–2.3	CKSHS2	
DNA segregation, mitosis, chromatin assembly			
D38751	–31.0	kinesin-like DNA binding protein (KID)	
U20979	–7.4	chromatin assembly factor-I p150 subunit	
U61145	–7.1	enhancer of Zeste homolog 2 (EZH2)	
D38553	–5.4	XCAP-H condensin homolog	Chang *et al*. (2000)
D63880	–4.2	KIAA0159	
X63692	–3.6	DNA (cytosin-5)-methyltransferase	
U09087	–3.4	thymopoietin β	
U18271	–3.4	thymopoietin	
U37426	–3.3	kinesin-like spindle protein (HKSP)	Ly *et al*. (2000)
X62534	–3.3	HMG2	Chang *et al*. (2000); Ly *et al*. (2000)
D38076	–3.3	RANBP1	Ly *et al*. (2000)
D00591	–3.2	RCC1	
L07515	–3.0	heterochromatin protein homologue (HP1)	
M34458	–2.9	lamin B	Chang *et al*. (2000)
X85137	–2.9	kinesin-related protein	
U14518	–2.7	centromere protein-A (CENP-A)	Chang *et al*. (2000); Ly *et al*. (2000)
M97856	–2.5	histone-binding protein	Ly *et al*. (2000)
X67155	–2.5	mitotic kinesin-like protein-1	Ly *et al*. (2000)
D80000	–2.5	SMC1L1	
D43948	–2.1	TOG	Ly *et al*. (2000)
DNA synthesis, replication			
L16991	–11.1	thymidylate kinase (CDC8)	Ly *et al*. (2000)
M87338	–8.7	replication factor C	
HG2379-HT3996	–8.5	serine hydroxymethyltransferase	
D55716	–5.7	P1CDC47/MCM7	Chang *et al*. (2000)
U40152	–3.5	origin recognition complex 1	Chang *et al*. (2000)
X52142	–3.1	CTP synthetase	
X59618	–2.7	ribonucleotide reductase M2 polypeptide	Chang *et al*. (2000)
M63488	–2.7	replication protein A 70 kDa subunit	
M15205	–2.6	thymidine kinase	Chang *et al*. (2000); Ly *et al*. (2000); Shelton *et al*. (1999)
U00238	–2.5	glutamine PRPP amidotransferase	
J04031	–2.5	MTHFD1	
U81375	–2.5	equilibrative nucleoside transporter 1 (hENT1)	
HG2846-HT2983	–2.3	dihydrofolate reductase	Chang *et al*. (2000)
X06745	–2.3	DNA polymerase α-subunit	Chang *et al*. (2000)
X54199	–2.2	GARS-AIRS-GART	
D84557	–2.2	MCM6	
Transcription, RNA processing, translation initiation			
X89416	–14.8	protein phosphatase 5	
D32002	–8.0	nuclear cap binding protein	
D12686	–7.1	eukaryotic initiation factor 4γ	
M85085	–6.6	cleavage stimulation factor	
U76421	–5.4	dsRNA adenosine deaminase DRADA2b	
X13482	–4.9	U2 snRNP-specific A′ protein	
X75918	–3.1	NOT	
U28042	–2.9	DEAD box RNA helicase-like protein	
M60784	–2.8	U1 snRNP-specific protein A	
U08815	–2.4	splicesomal protein (SAP61)	
L10838	–2.4	pre-mRNA splicing factor (SRP20)	Ly *et al*. (2000)
X67337	–2.2	HPBRII-4	
M86737	–2.2	high mobility group box (SSRP1)	
U90426	–2.1	nuclear RNA helicase	Ly *et al*. (2000)
L03532	–2.1	M4 protein	Ly *et al*. (2000)
Tumour suppressors			
X95152	–3.3	BRCA2	
L78833	–2.9	BRCA1	
U76638	–2.5	BARD1	Ly *et al*. (2000)
Telomerase component			
AF015950	–5.0	hTERT(*)	

The fold decrease shown represents the mean of four pairwise comparisons. A comprehensive list of all regulated genes can be found in the supplementary data. (*) Confirmed by TaqMan RT–PCR.

Table II. Transcriptional changes induced in NCI-H460 cells by long-term telomerase inhibitor treatment: up-regulation

Accession No.	Fold Δ	Gene name	Identified in context of senescence/ageing
Lysosomal proteins			
M16424	14.3	β-hexosaminidase α-chain	Lee *et al*. (1999, 2000)
M59916	10.9	acid sphingomyelinase (ASM)	
X62078	7.2	GM2 activator	
X78687	4.3	sialidase	
L09717	4.1	lysosomal membrane glycoprotein-2 (LAMP2)	
J03060	4.1	glucocerebrosidase (GCB)	
X52151	3.5	arylsulphatase A	
Z12173	3.2	glucosamine-6-sulfatase (GNS)	
X55079	3	GAA gene	Chang *et al*. (2000)
M95767	2.8	di-*N*-acetylchitobiase	
M22960	2.7	protective protein for β-galactosidase	
M29877	2.7	α-l-fucosidase	
D12676	2.6	lysosomal sialoglycoprotein	
U70063	2.5	acid ceramidase	
M63138	2.4	cathepsin D (CAT D)	Lee *et al*. (2000)
M34423	2.2	β-galactosidase (GLB1)	
Mitochondrial proteins			
M68840	10	monoamine oxidase A (MAOA)	
X05409	5.7	aldehyde dehydrogenase I ALDH I	
U54617	5.4	pyruvate dehydrogenase kinase isoform 4	
D87328	5	HCS	
M32879	3	steroid 11-β-hydroxylase (CYP11B1)	
D16481	2.2	3-ketoacyl-CoA thiolase β-subunit	
ECM/ECM signalling/cell adhesion			
L13923	6.5	fibrillin	
X17094	6.5	furin	
U47926	4.4	unknown protein B (homology to mGROS1)	
X03168	4.3	vitronectin	
U13896	3.9	homolog of *Drosophila* discs large protein, isoform 2	
M14648	3.3	vitronectin receptor α subunit	
U64573	3.2	connexin 43	
X52947	2.8	cardiac gap junction protein	
U59289	2.7	H-cadherin	
M61916	2.5	laminin B1 chain	Lee *et al*. (2000)
X68742	2.5	integrin α subunit	
HG2981-HT3125	2.4	Epican, alt. splice 1	
DNA structure			
X57129	10.3	H1.2 gene for histone H1	
X57985	9.5	GL105 gene for histones H2B.1 and H2A	
U90551	3.8	histone 2A-like protein (H2A/l)	
X60487	3.7	H4 histone family, member H	
Z29331	3.6	ubiqutin-conjugating enzyme UBCH2	
U40705	2.3	TRF1 (telomeric repeat binding factor-1)	
Complement, coagulation			
U92971	8.7	protease-activated receptor 3 (PAR3)	
J04080	4.2	complement C1r (multiple probe sets)	Ly *et al*. (2000); Lee *et al*. (2000)
M59499	3.5	lipoprotein-associated coagulation inhibitor (LACI)	
M14113	3.4	coagulation factor VIII:C	
M65292	3	factor H homologue	
Fatty acid oxidation/metabolism			
X14813	4.9	3-oxoacyl-CoA thiolase	
U46689	2.7	microsomal aldehyde dehydrogenase (ALD10)	
L40904	2.3	peroxisome proliferator activated receptor γ	
D16481	2.2	mitochondrial 3-ketoacyl-CoA thiolase β-subunit	
U03688	2.1	dioxin-inducible cytochrome P450 (CYP1B1)	Shelton *et al*. (1999)
Growth factors and cytokine signalling			
HG987-HT987	12.5	MAC25/IGFBP7	
M97936	11.1	STAT1 (multiple probe sets)	
M34057	8.3	transforming growth factor-β1 binding protein	
M62403	8.3	insulin-like growth factor binding protein 4 (*)	
M27288	7.5	oncostatin M	
U23070	6.4	putative transmembrane protein NMA (sim. to BAMBI)	
D37965	6.2	PDGF receptor β-like tumor suppressor (PRLTS)	
L20861	4.6	WNT5a (*)	
X04434	4.4	insulin-like growth factor I receptor	
D87258	3.5	cancellous bone osteoblast serin protease	Ly *et al*. (2000)
AB000584	3.3	TGF-β superfamily protein	Ly *et al*. (2000)
X62320	3.3	acrogranin (epithelin 1 and 2)	
Z29090	2.7	phosphatidylinositol 3-kinase	
X04571	2.3	kidney epidermal growth factor (EGF) precursor	
J04513	2.3	basic fibroblast growth factor (bFGF)	
HG3484-HT3678	2.2	CLK1 dual specificity kinase	
Cell cycle/ DNA damage response			
U09579	12.9	$p21^{MDA6/WAF1}$ (*)	Ly *et al*. (2000); Shelton *et al*. (1999)
U33203	2.3	MDM2-E	

(*) For explanation see footnote to Table I.

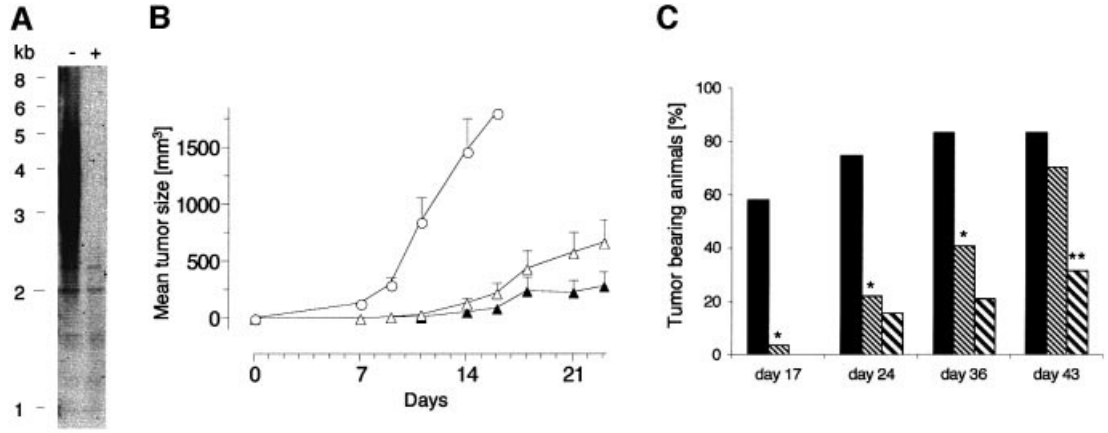

Fig. 6. Tumorigenicity assay. Nude mice were each injected with 1.5×10^6 HT1080 control or pre-senescent, telomere shortened cells. Tumour size was measured in regular intervals. (**A**) Telomere length of untreated control (–) and inhibitor-treated (+) HT1080 cells used to inject nude mice. (**B**) Mean tumour size of animals bearing control ($n = 24$) (open circles) and pre-senescent cells in the absence ($n = 27$) (open triangles) or presence ($n = 19$) (closed triangles) of BIBR1532. (**C**) The number of animals (as a percentage) with a tumour >1000 mm^3 for untreated control (black) and pre-treated cells in the absence (thin stripes) or presence (bold stripes) of BIBR1532 at the indicated days after injection. Statistical analysis was performed using Fisher's exact test, with significant differences ($p < 0.05$) between untreated control and pre-treated cells (*; $p < 0.0002$) as well as between pre-treated cells in the presence or absence of BIBR1532 (**; $p = 0.01034$) at the indicated time points.

biology or DNA damage response were found to be altered in their expression.

Effect of telomerase inhibition on tumorigenic potential

Telomerase is an unusually challenging target for demonstrating *in vivo* efficacy because of the long lag period required until telomeres are sufficiently shortened to produce detrimental effects on cell growth. The treatment of pre-established tumours with a telomerase inhibitor in standard mouse xenograft models will not result in a growth delay during the limited time a mouse can bear a fast-growing tumour xenograft. Thus, we attempted to create a model system expected to be more sensitive to inhibitor treatment by using tumour cells with sufficiently short telomeres. Since established tumour cell lines do not fulfil these criteria, we utilized inhibitor-treated, late-passage HT1080 fibrosarcoma cells with an average TRF size of only 1.6 kb (Figure 6A) but with an *in vitro* growth rate and colony forming ability similar to control cultures. After subcutaneous injection into immunodeficient mice, untreated control cells with telomeres of ~4 kb (Figure 6A) reached a detectable tumour size ($\geq$50 mm^2) in 4.53 ± 0.6 days ($n = 24$) whereas the telomere-shortened cells formed detectable tumours only after a lag period of 16.5 ± 1.8 days ($n = 27$, $p < 0.0001$). The average tumour size (Figure 6B) and incidence (Figure 6C) up to 36 days after injection was significantly lower in animals bearing pre-treated, telomere-shortened cells. This tumour model was also used to study *in vivo* inhibition of human telomerase. We treated mice carrying subcutaneous implants of the telomere-shortened HT1080 cells with BIBR1532 at a dose of 100 mg/kg/day orally beginning on the day of implantation. BIBR1532 is very specific and selective for human telomerase and inhibits mouse telomerase only with an IC_{50} >50 μM. Because of this 500-fold difference in potency, inhibition of host telomerase is not expected. The inhibitor treatment was very well tolerated with no signs of acute and chronic toxicity over the entire treatment period, which lasted 60 days for mice developing no or only small tumours. The lag-period to detectable tumour development was substantially prolonged to 26.2 ± 4.3 days ($n = 19$, $p = 0.0255$). Continued drug exposure inhibited initial tumour growth (Figure 6B) and resulted in a reduced incidence of tumours >1000 mm^3 with only six animals (32%) testing positive at day 43 of treatment compared to 19 animals (70%) not receiving the telomerase inhibitor ($p = 0.01034$, Figure 6C).

Discussion

A number of genetic validation experiments indicate that telomere maintenance by the enzyme telomerase is a key event in the immortalization process and the continuous proliferation of a large proportion of human cancers (Bodnar *et al*., 1998; Vaziri and Benchimol, 1998; Hahn *et al*., 1999a). The pharmacological results presented here demonstrate that extended propagation of human tumour cell lines in the presence of compounds from a novel class of selective, non-nucleosidic small molecule telomerase inhibitors results in progressive telomere shortening followed by the induction of a senescence phenotype and profound anti-proliferative effects *in vitro* and *in vivo*.

Several strategies to inhibit telomerase activity have been reported. These include peptide nucleic acids and 2′-O-MeRNA oligonucleotides directed towards the telomerase RNA template (Herbert *et al*., 1999), compounds that target telomeric DNA such as cationic porphyrins or anthraquinones (Sun *et al*., 1997) and nucleosidic reverse transcriptase inhibitors (Strahl and Blackburn, 1996). So far, these pharmacological strategies have had only limited success *in vivo* due to moderate efficacy or the inability of test compounds to penetrate cellular membranes under physiological conditions. Another approach described recently made use of dominant-negative alleles of hTERT, expression of which resulted in cell death of telomerase-positive cancer cell lines (Hahn *et al*., 1999b; Zhang *et al*., 1999). Although very effective and selective

in vitro, this gene therapy approach may not be readily applicable to the clinical setting.

The non-nucleosidic small molecule telomerase inhibitors described here overcome several of the past obstacles. Telomerase inhibition by BIBR1532 or BIBR1591 results in a continuous erosion of the telomeres in human cancer cell lines derived from fibrosarcoma, lung, breast and prostate carcinoma. No other cellular changes as assessed by morphological or gene expression parameters appear to be triggered by these selective drugs until the telomeres erode to a critically short length and the cells slow their growth. The phenotypic signs of senescence were observed not only in the p53-positive NCI-H460 cells but also in the p53-deficient HT1080, DU145 and MDA-MB231 cell lines, consistent with broad therapeutic utility. In contrast to previous results employing anti-sense oligonucleotides or the expression of dominant-negative hTERT alleles (Hahn *et al*., 1999b; Herbert *et al*., 1999; Zhang *et al*., 1999) we saw no evidence for an increased rate of apoptosis in the inhibitor-treated cells. This could be attributed to the different means employed to inhibit telomerase or to differences in the apoptotic potential of the non-overlapping set of cell lines used in these studies.

Changes that define age-related senescence of normal cells include enlarged and flattened morphology, increased granularity, expression of SA-β-GAL and multiple nuclei (Hayflick and Moorhead, 1961; Smith and Pereira-Smith, 1996). The senescence phenotype may be refined at the molecular level by comparing our list of regulated genes with that of a recent microarray study focusing on gene expression levels in replicative senescence of normal cells and age-related diseases (Chang *et al*., 2000; Ly *et al*., 2000). Many of the genes described in the physiological or premature ageing process, such as the down-regulation of mRNAs coding for cell cycle control proteins, proteins required for mitosis, DNA synthesis, replication and repair, are also found in the telomerase-inhibitor-treated, senescent NCI-H460 cancer cells and they may obey a programmed switch for mitotic events in senescent cells. A related feature of the inhibitor-treated NCI-H460 cells may be up-regulation of $p21^{Waf1}$, a cyclin-dependent kinase inhibitor whose induction triggers growth arrest associated with senescence and damage response. The similarities to the gene expression changes observed in recent array studies of p21-induced senescence (Chang *et al*., 2000) suggest that the senescent phenotype we observed upon telomerase inhibition may result, at least in part, from effects mediated by $p21^{Waf1}$.

The average TRF lengths in all inhibitor treated, senescent cells reach a size of only 1–2 kb at the onset of growth inhibition. A significant portion of these TRFs likely consists of subtelomeric sequences rather than TTAGGG repeats; suggesting that the true length of telomeric TTAGGG repeats has been reduced to only several hundred basepairs. Cytogenetic analysis indicates that some telomeres may even have lost all measurable TTAGGG repeats. Defective telomeres are unable to cap chromosomes effectively and the marked disarray in the genome of the inhibitor-treated cancer cell lines, including telomere loss and chromosomal end-to-end fusions, resembles the karyotypic changes in $mTERC^{-/-}$ mouse cells (Blasco *et al*., 1997). The role of telomerase in the immortalization of rodent cells may not be identical to human cells in all respects, but this mutant mouse model is extremely valuable for evaluating the biological consequences of telomerase inhibition. The lack of phenotypic effects in the early generation $mTERC^{-/-}$ mice suggests that general telomerase inhibition may be well tolerated with no severe toxic effects (Blasco *et al*., 1997). The ability of $mTERC^{-/-}$ mice to develop certain cancer types in later generations has been attributed to chromosome end-to-end fusions or the activation of telomerase-independent telomere maintenance mechanisms (Blasco *et al*., 1997; Greenberg *et al*., 1999; Rudolph *et al*., 1999). A similar ALT mechanism has been described for virus-transformed human cells and a small proportion of established human cancer cell lines that lack telomerase activity (Bryan *et al*., 1995). We have never observed induction of the ALT phenotype in any of the cell lines used in our studies. Induction of ALT has also never been reported in previous publications using other means of telomerase inhibition (Hahn *et al*., 1999b; Herbert *et al*., 1999; Zhang *et al*., 1999). A recent analysis of telomeric recombination mechanisms, which are apparently the mechanistic basis for ALT, suggests that telomere-positive cells may not possess a telomere maintenance mechanism other than telomerase (Dunham *et al*., 2000).

Recent data suggest that in $mTERC^{-/-}$ mouse cells telomere dysfunction is a prominent trait that impairs DNA repair and enhances sensitivity to ionizing radiation (Wong *et al*., 2000). This link between telomerase inhibition and radiosensitivity may provide a basis for further studies employing a combination of telomerase inhibitors and radiotherapeutic strategies for cancer treatment. In a clinical setting, the most likely use of telomerase inhibitors would be as an adjuvant treatment in combination with surgery, radiation treatment and conventional chemotherapy. Another potential application would be post-remission therapy in order to eliminate minimal residual disease.

Although an analysis of telomere lengths in primary tumours suggests that tumour telomeres are usually short, predicting that the phenotypic lag may be limited, we nevertheless expect that oral treatment may have to be administered continuously for weeks to months. Therefore, the success of a telomerase inhibitor therapy requires that compounds should be sufficiently well tolerated, have a low toxicity profile and are easy to administer. The compounds described here fulfil many of the required criteria and further studies with continued treatment *in vivo* are needed to determine the best candidates to study for clinical efficacy. At the very least, our discovery of a highly potent and selective class of telomerase inhibitors highlights the potential of targeting this enzyme in a mechanism-based approach to the development of new treatment modalities in cancer.

Materials and methods

Enzyme assays

Telomerase activity assays to determine the IC_{50} curves were performed and quantified using a PCR-based protocol followed by a TCA precipitation step (Schnapp *et al*., 1998). The total amount of incorporated [^{33}P]dCMP was measured by liquid scintillation counting and normalized to the control. As a source for telomerase, nuclear extracts derived from HeLa cells were used. For the direct telomerase assay, telomerase was reconstituted with insect cell expressed hTERT and *in vitro* transcribed

hTR as described (Wenz *et al*., 2001). Taq polymerase activity was determined as described by the manufacturer (Promega). The activity of DNA polymerases present in HeLa nuclear extracts (40 µg of total protein) was assayed under the following conditions: 20 mM Tris–HCl pH 7.9, 8 mM $MgCl_2$, 50 mM KCl, 0.5 mg/ml bovine serum albumin, 5 mM dithiothreitol, 2 mM spermidine, 80 µM each of dGTP, dCTP and TTP, 5 µM [α-^{32}P]dATP (3.6 Ci/mmol) and either 4 µg activated calf thymus DNA (Pharmacia) or 2 µg of poly A(dT) (Biotech) as template. Reactions were incubated for 30 min at 37°C and the radioactivity present in trichloroacetic acid precipitates collected on class-fibre filters was determined by liquid scintillation counting. Purified pure calf thymus DNA polymerase was obtained from Professor N.C.Brown (University of Massachusetts Medical School, Worcester) and Cambio (Cambridge, UK) and was assayed in the presence of 4 µg of activated calf thymus DNA as described above. Human RNA polymerase I was purified from HeLa nuclear extracts and assayed as described (MonoQ fraction, Schnapp and Grummt 1996). The activity of human RNA polymerases I, II and III was also assayed in HeLa nuclear extracts in the presence of 200 µg/ml α-amanitin using the same conditions. The activity of RNA polymerase II and III was calculated from the difference of the non-inhibited versus the α-amanitin-inhibited extract. *In vitro* translation assays were performed in the rabbit reticulocyte system as described by the manufacturer (Promega). *Escherichia coli* helicase I (Amersham) and pcTA Helicase from *Bacillus stearothermophilus* (Cambio) were assayed in the helicase ^{3}H SPA enzyme assay system as described by the manufacturer (Amersham). HIV1 reverse transcriptase was tested in the reverse transcriptase SPA enzyme assay (Amersham).

Cell lines

The lung cancer cell line NCI-H460, the fibrosarcoma cell line HT1080, the breast cancer cell line MDA-MB231 and the prostate cancer cell line DU145 were maintained in RPMI supplemented with 5 or 10% fetal calf serum in 5% CO_2 at 37°C. The cells were grown in 24-well tissue culture plates and replated every 2–3 days to ensure log-phase growth. The culture medium contained 10 µM of BIBR1532 or 50 µM of BIBR1591 dissolved in 0.1% DMSO and was replenished at every replating step or every 2–3 days for slower growing cells. The compounds were stable under these conditions. Control cells were untreated or treated with corresponding solvent concentrations. Cell growth and viability in the 7 day cytotoxicity study was determined using the tetrazolium dye assay.

Isolation of cellular DNA and telomere length analysis

Cell samples (2×10^6 cells) were harvested, washed and resuspended in DNazol (Life Technologies). Total cellular DNA was extracted according to the manufacturer's protocol. To measure telomere length, genomic DNA was digested with restriction enzymes *Hin*fI and *Rsa*I, fractionated on 0.6% agarose gel and transferred onto a nylon membrane. Telomere sequences were detected by hybridization with a synthetic oligonucleotide probe $(CCCTAA)_3$ end-labelled with fluorescein-dUTP. Detection relies on an anti-fluorescein-antibody conjugated to alkaline phosphatase (Amersham).

Cellular Assays

SA-β-galactosidase activity was detected as described (Dimri *et al*., 1995). For cell cycle analysis, cells were fixed with 2% paraformaldehyde for 20 min at room temperature and permeabilized with 0.25% Triton X-100 in phosphate-buffered saline by incubation for 5 min on ice. Cells were pelleted by centrifugation (1000 *g*, 5 min, 4°C), resuspended in propidium iodine staining buffer (0.1% RNase, 10 µg/ml propidium iodine in PBS) and incubated for 20 min at room temperature. The DNA content was analysed using a FACS Calibur (Becton Dickinson, Heidelberg, Germany). TUNEL assay was performed according to the manufacturer's protocol (Pharmingen, Heidelberg, Germany).

Fluorescence in situ hybridization and quantitative image analysis

Individual telomere length was analysed by quantitative fluorescence *in situ* hybridization (Q-FISH) as described previously (Martens *et al*., 1998, 2000). Digital images of metaphase spreads were recorded with a digital camera (Sensys, Photometrics) on a Zeiss Axioplan II fluorescence microscope using the Vysis workstation QUIPS. Telomere profiles were analysed by the TFL-TELO software (Poon *et al*., 1999). Telomere fluorescence intensity values were expressed in arbitrary units.

Analysis of gene expression using oligonucleotide arrays

Total RNA was extracted from frozen cell pellets by using Trizol reagent (Life Technologies). RNA was purified on RNeasy Mini columns (Qiagen) for RNA cleanup and DNase treatment (RNase-Free DNase Set Protocol, Qiagen). RNA was converted into double-stranded cDNA by using the Superscript Choice System (Life Technologies). Biotin-labelled cRNA synthesis was carried out using 10 µg of total RNA according to the Affymetrix technical manual (Lockhart *et al*., 1996; Fambrough *et al*., 1999). Hybridization, washing, staining, and scanning of Affymetrix Genechip HuGeneFL oligonucleotide arrays (Affymetrix) was carried out according to the Affymetrix technical manual (Lockhart *et al*., 1996; Fambrough *et al*., 1999) in an Affymetrix hybridization oven and fluidics station and a Hewlett-Packard GeneArray Scanner. Data analysis was performed using Affymetrix software. Expression levels of untreated or DMSO-treated control cells were compared with expression levels of cells treated with the telomerase inhibitor BIBR1591. Four pairwise comparisons were calculated by comparing two unrelated sets of cells grown with BIBR1591 to either untreated NCI-H460 cells or to cells treated with DMSO as a solvent control. Selected genes were required to show at least a 2-fold regulation in at least three out of four pairwise comparisons.

Quantitative RT–PCR

We used the same RNA preparations for both microarray and quantitative RT–PCR analyses. mRNA quantitation was performed using the TaqMan EZ RT–PCR kit (PE Applied Biosystems) and all samples were analysed in triplicates on the ABI PRISM 7700 Sequence Detection System (PE Applied Biosystems). Gene-specific oligonucleotide probes with 5′-fluorescent and 3′-rhodamine (quench) tags were designed for hTERT, Wnt5a, IGFBP4, $p21^{Waf1}$, cyclin A, and GAPDH as an internal standard. PCR conditions as well as sequences of RT–PCR primers and probes will be provided on request.

Tumorigenicity assays

The ability of untreated and inhibitor treated HT1080 fibrosarcoma cells to form tumours was determined by injecting 1.5×10^6 cells subcutaneously in immunodeficient nu/nu NMRI mice. BIBR1532 was prepared in a vehicle of 20% cremophore RH40, 80% water with equimolar amounts of NaOH. Treatment was administered by gavage. Growth of the tumours was recorded by calliper measurements determining length and width of the palpatable, subcutaneous tumour mass three times per week.

Supplementary data

Supplementary data for this paper are available at *The EMBO Journal* Online.

Acknowledgements

We thank the members of the Department of Oncology Research for helpful discussions and encouragement, Dr Uwe Bamberger for help with the animal experiments and Josef Eiband, Herbert Fischbach and Michael Koehler for excellent technical assistance. M.P. and U.M.M. were supported by the Deutsche Forschungsgemeinschaft (SFB364). Work in J.L.'s laboratory was supported in part by the Swiss National Science Foundation and the Fifth Framework Program of the European Union (via the Bundesamt fuer Bildung und Wissenschaft, Bern).

References

Blackburn,E. and Greider,C. (eds) (1995) *Telomeres*. Cold Spring Harbor Laboratory Press, Cold Spring Harbor, New York, NY.

Blasco,M.A., Lee,H.W., Hande,M.P., Samper,E., Lansdorp,P.M., DePinho,R.A. and Greider,C.W. (1997) Telomere shortening and tumour formation by mouse cells lacking telomerase RNA. *Cell*, **91**, 25–34.

Bodnar,A.G. *et al.* (1998) Extension of life-span by introduction of telomerase into normal human cells. *Science*, **279**, 349–352.

Bryan,T.M., Englezou,A., Gupta,J., Bacchetti,S. and Reddel,R.R. (1995) Telomere elongation in immortal human cells without detectable telomerase activity. *EMBO J.*, **14**, 4240–4248.

Chang,B.D., Watanabe,K., Broude,E.V., Fang,J., Poole,J.C., Kalinichenko,T.V. and Roninson,I.B. (2000) Effects of $p21^{Waf1/Cip1/Sdi1}$ on cellular gene expression: implications for carcinogenesis, senescence, and age-related diseases. *Proc. Natl Acad. Sci. USA*, **97**, 4291–4296.

Cooke,H.J. and Smith,B.A. (1986) Variability at the telomeres of the

human X/Y pseudoautosomal region. *Cold Spring Harbor Symp. Quant. Biol.*, **51**, 213–219.

Counter,C.M., Avilion,A.A., LeFeuvre,C.E., Stewart,N.G., Greider,C.W., Harley,C.B. and Bacchetti,S. (1992) Telomere shortening associated with chromosome instability is arrested in immortal cells which express telomerase activity. *EMBO J.*, **11**, 1921–1929.

Counter,C.M., Botelho,F.M., Wang,P., Harley,C.B. and Bacchetti,S. (1994) Stabilization of short telomeres and telomerase activity accompany immortalization of Epstein–Barr virus-transformed human B lymphocytes. *J. Virol.*, **68**, 3410–3414.

Dimri,G.P. *et al.* (1995) A biomarker that identifies senescent human cells in culture and in ageing skin *in vivo*. *Proc. Natl Acad. Sci. USA*, **92**, 9363–9367.

Dunham,M.A., Neumann,A.A., Fasching,C.L. and Reddel,R.R. (2000) Telomere maintenance by recombination in human cells. *Nature Genet.*, **26**, 447–450.

Fambrough,D., McClure,K., Kazlauskas,A. and Lander,E.S. (1999) Diverse signaling pathways activated by growth factor receptors induce broadly overlapping, rather than independent, sets of genes. *Cell*, **97**, 727–741.

Feng,J.L. *et al.* (1995) The RNA component of human telomerase. *Science*, **269**, 1236–1241.

Greenberg,R.A., Chin,L., Chin,L., Femino,A., Lee,K.H., Gottlieb,G.J., Singer,R.H., Greider,C.W. and DePinho,R.A. (1999) Short dysfunctional telomeres impair tumorigenesis in the INK4aΔ2/3 cancer-prone mouse. *Cell*, **97**, 515–525.

Hahn,W.C., Counter,C.M., Lundberg,A.S., Beijersbergen,R.L., Brooks, M.W. and Weinberg,R.A. (1999a) Creation of human tumour cells with defined genetic elements. *Nature*, **400**, 464–468.

Hahn,W.C. *et al.* (1999b) Inhibition of telomerase limits the growth of human cancer cells. *Nature Med.*, **5**, 1164–1170.

Harley,C.B. (1991) Telomere loss: mitotic clock or genetic time bomb? *Mutat. Res.*, **256**, 271–282.

Harley,C.B., Futcher,A.B. and Greider,C.W. (1990) Telomeres shorten during ageing of human fibroblasts. *Nature*, **345**, 458–460.

Harrington,L., Zhou,W., McPhail,T., Oulton,R., Yeung,D.S.K., Mar,V., Bass,M.B. and Robinson,M.O. (1997) Human telomerase contains evolutionarily conserved catalytic and structural subunits. *Genes Dev.*, **11**, 3109–3115.

Hastie,N.D., Dempster,M., Dunlop,M.G., Thompson,A.M., Green,D.K. and Allshire,R.C. (1990) Telomere reduction in human colorectal carcinoma and with ageing. *Nature*, **346**, 866–868.

Hayflick,L. and Moorhead,P. (1961) The serial cultivation of human diploid cell strains. *Exp. Cell Res.*, **25**, 585–621.

Herbert,B.S., Pitts,A.E., Baker,S.I., Hamilton,S.E., Wright,W.E., Shay,J.W. and Corey,D.R. (1999) Inhibition of human telomerase in immortal human cells leads to progressive telomere shortening and cell death. *Proc. Natl Acad. Sci. USA*, **96**, 14276–14281.

Kim,N.W. *et al.* (1994) Specific association of human telomerase activity with immortal cells and cancer. *Science*, **266**, 2011–2015.

Lee,C.K., Klopp,R.G., Weindruch,R. and Prolla,T.A. (1999) Gene expression profile of aging and its retardation by caloric restriction. *Science*, **285**, 1390–1393.

Lee,C.K., Weindruch,R. and Prolla,T.A. (2000) Gene-expression profile of the ageing brain in mice. *Nature Genet.*, **25**, 294–297.

Lockhart,D.J. *et al.* (1996) Expression monitoring by hybridization to high-density oligonucleotide arrays. *Nature Biotechnol.*, **14**, 1675–1680.

Ly,D.H., Lockhart,D.J., Lerner,R.A. and Schultz,P.G. (2000) Mitotic misregulation and human ageing. *Science*, **287**, 2486–2492.

Martens,U.M., Zijlmans,J.M., Poon,S.S., Dragowska,W., Yui,J., Chavez,E.A., Chavez,E.A., Ward,R.K. and Lansdorp,P.M. (1998) Short telomeres on human chromosome 17p. *Nature Genet.*, **18**, 76–80.

Martens,U.M., Chavez,E.A., Poon,S.S., Schmoor,C. and Lansdorp,P.M. (2000) Accumulation of short telomeres in human fibroblasts prior to replicative senescence. *Exp. Cell. Res.*, **256**, 291–299.

Meyerson,M. *et al.* (1997) hEST2, the putative human telomerase catalytic subunit gene, is up-regulated in tumour cells and during immortalization. *Cell*, **90**, 785–795.

Morin,G.B. (1989) The human telomere terminal transferase enzyme is a ribonucleoprotein that synthesizes TTAGGG repeats. *Cell*, **59**, 521–529.

Nakamura,T.M., Nakamura,T.M., Morin,G.B., Chapman,K.B., Weinrich, S.L., Andrews,W.H., Lingner,J., Harley,C.B. and Cech,T.R. (1997) Telomerase catalytic subunit homologs from fission yeast and human. *Science*, **277**, 955–959.

Poon,S.S., Martens,U.M., Ward,R.K. and Lansdorp,P.M. (1999) Telomere length measurements using digital fluorescence microscopy. *Cytometry*, **36**, 267–278.

Rudolph,K.L., Rudolph,K.L., Chang,S., Lee,H.W., Blasco,M., Gottlieb,G.J., Greider,C. and DePinho,R.A. (1999) Longevity, stress response, and cancer in aging telomerase-deficient mice. *Cell*, **96**, 701–712.

Schnapp,A. and Grummt,I. (1996) Purification, assay, and properties of RNA polymerase I and class I-specific transcription factors in mouse. *Methods Enzymol.*, **273**, 233–248.

Schnapp,G., Rodi,H.P., Rettig,W.J., Schnapp,A. and Damm,K. (1998) One-step affinity purification protocol for human telomerase. *Nucleic Acids Res.*, **26**, 3311–3313.

Shay,J.W. and Bacchetti,S. (1997) A survey of telomerase activity in human cancer. *Eur. J. Cancer*, **33**, 787–791.

Shelton,D.N., Chang,E., Whittier,P.S., Choi,D. and Funk,W.D. (1999) Microarray analysis of replicative senescence. *Curr. Biol.*, **9**, 939–945.

Smith,J.R. and Pereira-Smith,O.M. (1996) Replicative senescence: implications for *in vivo* ageing and tumour suppression. *Science*, **273**, 63–67.

Strahl,C. and Blackburn,E.H. (1996) Effects of reverse transcriptase inhibitors on telomere length and telomerase activity in two immortalised human cell lines. *Mol. Cell. Biol.*, **16**, 53–65.

Sun,D.Y., Thompson,B., Cathers,B.E., Salazar,M., Kerwin,S.M., Trent,J.O., Jenkins,T.C., Neidle,S. and Hurley,L.H. (1997) Inhibition of human telomerase by a G-quadruplex-interactive compound. *J. Med. Chem.*, **40**, 2113–2116.

Vaziri,H. and Benchimol,S. (1998) Reconstitution of telomerase activity in normal human cells leads to elongation of telomeres and extended replicative life span. *Curr. Biol.*, **8**, 279–282.

Wenz,C., Enenkel,B., Amacker,M., Kelleher,C., Damm,K. and Lingner,J. (2001) Human telomerase contains two cooperating telomerase RNA molecules. *EMBO J.*, **20**, 3526–3534.

Wong,K.K. *et al.* (2000) Telomere dysfunction impairs DNA repair and enhances sensitivity to ionising radiation. *Nature Genet.*, **26**, 85–88.

Zhang,X.L., Mar,V., Zhou,W., Harrington,L. and Robinson,M.O. (1999) Telomere shortening and apoptosis in telomerase-inhibited human tumour cells. *Genes Dev.*, **13**, 2388–2399.

Received September 11, 2001; revised October 23, 2001; accepted October 26, 2001